

The Parkfield, California earthquake experiment: An update in 2000

Evelyn Roeloffs

US Geological Survey, 5400 MacArthur Blvd., Vancouver, WA 98661, USA

The US Geological Survey, in cooperation with other institutions, continues to monitor the San Andreas Fault (SAF) near Parkfield, California, hoping to capture high resolution records of continuous deformation before, during and after a magnitude 6 earthquake, as well as the details of its rupture initiation and strong ground motion. Despite the failure of the prediction that the next M 6 Parkfield earthquake would occur before 1993, Parkfield still has a higher known probability (1 to 10% per year) than anywhere else in the US of a M 6 or greater earthquake. Parkfield instrumentation is still largely in place, although there have been losses due to attrition as well as improvements made possible by new technology. Most Parkfield data sets are now available via the Internet, and all others may be obtained upon request from individual investigators. Detailed seismic monitoring has shown that events with identical seismograms, recurring in exactly the same locations, account for a high proportion of the background seismicity at Parkfield. Geophysical studies have revealed that fault zone seismic and electrical properties are consistent with high fluid content. The rate of interseismic slip on the SAF changed significantly in late 1992 or early

1993, during a period of relatively high seismic activity. The strain-rate change, measured by borehole tensor strainmeters and the two-colour electronic distance-measuring network, was also manifested as shortened recurrence intervals of repeating micro-earthquakes. Whether or not the accelerated deformation turns out to be an intermediate-term precursor to the next M 6 Parkfield earthquake, documenting the variation of interseismic strain rates with time has important implications for fault dynamics and seismic hazard estimation. Two possible instances of pre-earthquake signals have been recorded at Parkfield: water-level and strain changes over a period of three days prior to the nearby 1985 M_w 6.1 Kettleman Hills, California, earthquake and anomalous electromagnetic signals prior to the M 5 earthquake near Parkfield on 20 December 1994. Future work planned at Parkfield includes a National Science Foundation proposal to construct an SAF Observatory at Depth (SAFOD), as part of the Earthscope initiative. The Observatory will consist of a 4-km-deep borehole to penetrate the SAF and a shallow micro-earthquake cluster on Middle Mountain, directly above the hypocenter of the 1966 Parkfield earthquake.

1. Introduction

The US Geological Survey (USGS), in partnership with the state of California and other institutions, has intensively monitored the San Andreas Fault (SAF) near the town of Parkfield since 1985 (Figure 1). One goal is to obtain a detailed long-term record of fault behaviour believed likely to culminate in a moderate earthquake. Another goal is to record the details of seismic rupture, strong ground motion, and earthquake effects. Roeloffs and Langbein¹ described the experiment's instrumentation and findings as of 1993. Currently (April 2000), the anticipated M 6 earthquake that the experiment was designed to record has not yet occurred. Seven years have elapsed since expiration of the original prediction, which stated that the next M 6 Parkfield earthquake would take place with 95% confidence before 1993 (ref. 2). Although many still regard the Parkfield experiment as a critical opportunity to observe an active fault as it loads to

failure in a moderate earthquake, there is controversy as to how long the experiment should continue, and at what expense.

This article, an update of Roeloffs and Langbein¹, summarizes current thinking about the likelihood of future Parkfield earthquakes and describes changes to the field instrumentation as technology has improved and funding has fallen. There is strong evidence for a change in the rate of aseismic fault slip at Parkfield in 1992 or 1993. Recognition of clustering in background micro-seismicity and geophysical indicators of fault zone fluids are important new findings about the SAF. Funding has been requested for a 4-km-deep drillhole to penetrate the SAF near Parkfield and sample fault zone rocks and fluids, as well as provide an observatory for fault zone observations at depth.

2. Parkfield earthquake probabilities

Since the expected M 6 Parkfield earthquake did not occur prior to 1993, revised annual probabilities for the

e-mail: evelynr@usgs.gov

next such event have been suggested, most of which are summarized in Roeloffs and Langbein¹. In a more recent study, Kagan³ computed probabilities of sequences like those of the historic Parkfield earthquakes, and concluded that the observed sequence was not inconsistent with the assumption that earthquakes occur according to a Poisson, rather than quasi-periodic, model. This analysis puts the annual probability of a Parkfield mainshock at about 1%. A review of all available studies⁴ concluded that 10% was a consensus value for the annual probability, and judged this probability high enough to recommend continuing the experiment.

The Parkfield experiment includes a computerized system for detecting unusual signals in the monitoring data, allowing the USGS to alert the California Office of Emergency Services if tectonic events indicate that the next $M 6$ Parkfield earthquake might be imminent. Four levels of alert exist, the highest (level 'A') reachable only by rapid aseismic creep or a potential large foreshock, corresponding to an estimated 37% probability of the mainshock occurring within three days.

Michael and Jones⁵ provide new estimates of Parkfield seismic alert probabilities, based on lower estimates of the annual mainshock probability (4 to 10%), a better data set for estimating background seismicity, and a revised methodology⁶. They also propose a new definition of the Parkfield mainshock as any event with $M_w \geq 5.7$, accompanied by surface rupture, whose epicenter is within 5 km of the mapped fault trace between the latitudes of $35^{\circ}45' N$ and $36^{\circ} N$. They suggest that Parkfield foreshocks should be considered capable of occurring anywhere within a 'Parkfield box', which extends along

the same length of the SAF as the zone specified to contain the mainshock, but is twice as wide. With these definitions, the probability of a mainshock with epicenter in the specified area, given the occurrence of a $M > 5$ potential foreshock, is between 2.2 and 19%, depending upon possible variations in annual mainshock probability and form of the dependence of foreshock probabilities on magnitude. A potential foreshock at Parkfield could now only produce a level 'A' alert if special studies of the waveform and hypocenter were to show it to be a recurrence of the immediate foreshock to the 1934 and 1966 Parkfield earthquakes. A $M 5$ foreshock preceded each of those events by 17 minutes, and these 1934 and 1966 foreshocks had essentially identical seismograms⁷. Recognizing a future $M 5$ event as a repeat of one of these foreshocks would currently require more time than 17 minutes, implying that a level 'A' alert is unlikely to be issued.

Although the probability that the Parkfield earthquake will occur in any given year has been revised downward, it is still the location of highest known probability for a moderate earthquake anywhere in California, and has one of the shortest recurrence intervals, based on the same methods used to estimate earthquake probabilities elsewhere in the state. In 1857, $M 6$ earthquakes on the SAF near Parkfield were followed within 2 hours by the great 1857 Fort Tejon, California, earthquake ($M 7.9$)⁸, suggesting that a future Parkfield event might herald a damaging earthquake in now densely-populated southern California. On the other hand, the anticipated Parkfield earthquake is not believed likely to cause fatalities or significant financial losses by itself. Level funding for earthquake studies in the US, increased emphasis since the 1994 Northridge, California earthquake on research with short-term hazard mitigation payoffs, and uncertainty about the likelihood of the next Parkfield earthquake have made the issues of how long the experiment should continue, and at what cost, important ones to critically review.

3. Instrumentation status

The instrumentation at Parkfield includes seismic networks, crustal deformation sensors, and several arrays of strong-motion instruments. The strong-motion instrumentation remains essentially as described in Roeloffs and Langbein¹, but other networks have undergone some change.

Two borehole volumetric strainmeters (dilatometers) have ceased to operate and have not been replaced, leaving five functional dilatometers. The EDT borehole tensor strainmeter (BTSM) still operates close to the location of one of the non-operational dilatometers.

The southernmost creepmeter, X461, has been decommissioned. Groundwater radon, soil hydrogen, shallow borehole tilt, and borehole microtemperature are no longer measured. Two groundwater-level monitoring

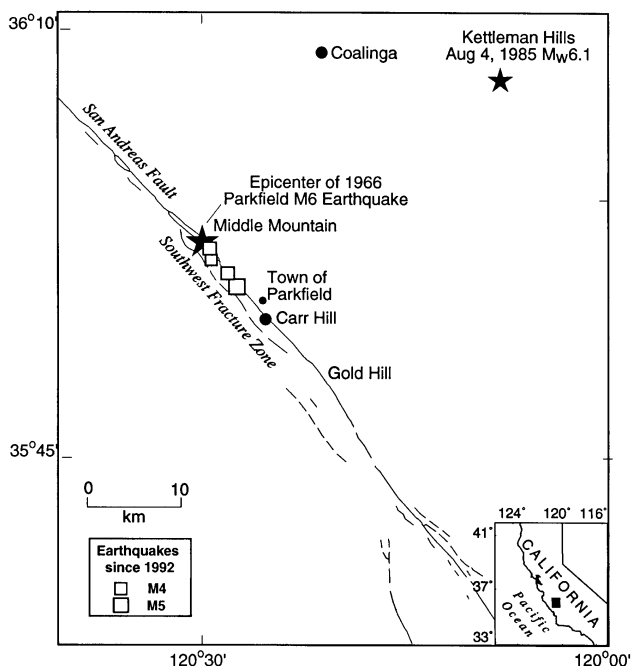


Figure 1. Map of the Parkfield area.

wells were abandoned, and the former radon-monitoring well at Carr Hill was converted to a groundwater-level observation site in 1994. With these changes, eight groundwater-level monitoring sites are still operating, including one well in which the water-level is monitored at two depths.

The two-colour electronic distance-measuring (EDM) network continues to be measured at a reduced frequency of six times per month. It is currently supplemented by continuous GPS observations along several of its baselines, and the continuous GPS is envisioned to replace the two-colour EDM network eventually.

The downhole High Resolution Seismic Network (HRSN) is being upgraded with new electronics, and three new stations will be added near the proposed deep drillhole (see Section 6). The controlled-waveform-monitoring experiment has been discontinued for lack of funds. Two new broadband seismic stations have been installed in the Parkfield area.

The resistivity and magnetic monitoring networks have been upgraded, but funding difficulties make their future uncertain. There are two magnetic monitoring sites. A vertical coil is monitored at one site, and at the other site three orthogonal coils and two orthogonal dipoles allow all non-zero components of the magnetic and electrical fields to be monitored in the frequency range from 10^{-4} to 20 Hz. Data are digitized with 20-bit precision at 40 Hz and 1 Hz and are sent by telemetry to the Northern California Earthquake Data Center (NCEDC), in contrast to the previous practice in which only average values of the magnetic fields in certain frequency bands were retained. Improved data-processing techniques were implemented so that long-period magnetic signals of upper atmospheric origin could be identified by comparison with a similar station near Hollister⁹. The electrical dipoles would permit detection of any possible 'Seismic Electrical Signals' similar to those reported by Varotsos *et al.*¹⁰, and the magnetic data would help clarify the mechanisms of such signals. The magnetic coils are also designed to detect signals similar to those recorded by Fraser-Smith *et al.*¹¹ prior to the Loma Prieta earthquake. Data from the Parkfield resistivity network¹² are now also digitized at the same rates as the magnetic data.

Many types of data from Parkfield can now be viewed or downloaded via Internet. The USGS Parkfield home

page (<http://quake.wr.usgs.gov/QUAKES/Parkfield/>) contains links to plots of crustal deformation data. Parkfield earthquakes recorded by the surface short-period network are part of the Northern California Earthquake Catalogue, accessible at the NCEDC, operated by the USGS and the University of California at Berkeley. Data from broadband seismometers and the downhole HRSN are also available at the NCEDC. Work is currently underway to place all Parkfield deformation data at the NCEDC, where it will be available to the entire scientific community. In the meantime, most Parkfield data may be obtained on request by contacting individual investigators.

4. Discoveries about the SAF at Parkfield

The large amount of detailed data collected at Parkfield has yielded new insights about microseismicity patterns and fault structure. Many of these findings are consistent with a role for fluids in controlling fault behaviour.

4.1 Repeating earthquakes

Independent analyses by two groups have shown that, at Parkfield, earthquakes with $M > 4$, as well as microearthquakes with $M_w < 1.3$, occur largely in earthquake families, or clusters, of recurring events with identical seismograms.

It has long been known that foreshocks 17 minutes before each of the 1934 and 1966 $M 6$ Parkfield earthquakes produced nearly identical Wood-Anderson seismograms near Berkeley, California⁷. This phenomenon is the basis for the current level 'A' alert criterion, which requires an earthquake whose seismogram matches that of the 1934 and 1966 foreshocks. Ellsworth and others^{13,14} have extended this intriguing observation to show that almost all $M > 4$ earthquakes near Parkfield can be grouped into classes, each characterized by a distinctive seismogram and presumably repeatedly rupturing the same small fault patch despite the occurrence of two $M 6$ earthquakes. Two of the four $M > 4$ earthquakes since 1992 (EQ1 and EQ3 in Table 1) have fit formal criteria for potential Parkfield foreshocks (and prompted public warnings that a $M 6$ event was temporarily more likely). Closer scrutiny showed seismograms of EQ3, in

Table 1. Earthquakes $M > 4$ in Parkfield since 1986, from the University of California at Berkeley/US Geological Survey Northern California Earthquake Data Center. Coda magnitudes were obtained from the NCEDC. Other studies have assigned different, usually higher magnitudes to these events, so to avoid confusion they will be referred to as EQ1 to EQ4

Earthquake	Date	Time (UT)	Latitude	Longitude	Depth (km)	Magnitude (coda)
EQ1	1992/10/20	05:28:08.90	35.9285°N	120.4728°W	10.21	4.3
EQ2	1993/04/04	05:21:25.27	35.9413°N	120.4925°W	7.65	4.2
EQ3	1993/11/14	12:25:34.87	35.9527°N	120.4968°W	11.70	4.6
EQ4	1994/12/20	10:27:47.17	35.9175°N	120.4643°W	9.10	4.7

November 1993, to be identical to those from a foreshock three days prior to the 1966 Parkfield mainshock. None of the events in Table 1 has been a repeat of the 17-minute foreshocks, however.

The downhole HRSN at Parkfield has recorded microseismicity on this stretch of the fault for 11 years at a level of detail unsurpassed anywhere worldwide. Nadeau *et al.*¹⁵ showed that about half of the events recorded by the HRSN with $0.2 < M_w < 1.3$ occur in about 300 clusters of microearthquakes with highly similar waveforms. Within clusters, relative event locations based on waveform cross-correlation can be accurate to within 5 m (ref. 16). Many of these clusters have characteristic recurrence times that scale with the magnitude of the repeating events. Changes in this recurrence time have been exploited, as described later, to infer that slip rates over portions of the fault vary with time. Since the clusters cannot be detected without low-noise data and special data-processing techniques, it remains unknown whether other parts of the SAF also exhibit the clustering behaviour. Tullis¹⁷ suggests that the microearthquake clusters may represent lithologically distinct sites that have velocity-weakening frictional behaviour. Boatwright and Cocco¹⁸ point out that the fault planes can be divided into zones based on their tendency for either seismic rupture, aftershocks, or background seismicity, suggesting that a mix of velocity-weakening and velocity-strengthening behaviour is distributed within the part of the fault zone that is macroscopically creeping with localized patches of background seismicity. The picture emerging from all of these studies is that background seismicity at Parkfield repeatedly ruptures the same tiny areas of the fault, which seem to have unique properties that control the SAF's behaviour.

4.2 Role of fluids

Fault-zone fluids are widely believed key to understanding earthquake generation. Specifically, it has been hypothesized that high fluid pressure in the fault zone is the mechanism that reduces the frictional strength of the fault zone, and that time variations in fluid pressure control the timing of earthquakes (e.g. Miller *et al.*¹⁹). Some of the data collected at Parkfield now allow the feasibility of these hypotheses to be tested.

Several studies of seismic wave velocities around Parkfield have identified bodies at seismogenic depths with velocities or attenuation that could be caused by high fluid pressure. Between depths of 6 and 10 km, there is a 3-km-wide zone of low V_p (ref. 20), relatively lower V_s , and therefore high V_p/V_s (1.9–2.0) (ref. 21) immediately north-east of the active fault surface as defined by microseismicity. Along strike of the SAF, this body extends from the 1966 hypocentre about 5 km to the south-east^{21,22}. This zone is also characterized by high

attenuation. The seismic wave propagation characteristics of this body are consistent with high fluid content, but do not require pressure in the fluid to be elevated. High fluid pressure in a 1-km-deep borehole on the NE side of the SAF in this area, however, shows that there is at least localized overpressure at depth.

Unsworth *et al.*²³ conducted a magnetotelluric transect across the SAF on Middle Mountain, directly above the north-eastern limit of the high V_p/V_s body. The prominent finding is a vertical zone of low resistivity along the fault trace, about 500 m wide, extending to about 4000 m depth, with higher resistivities, or narrower width, at greater depth. This zone contains significant areas where the resistivity is about $1 \Omega - m$, a range too low to be reached through the presence of clays or serpentinite alone, and therefore strongly indicates a network of interconnected pore space. Unsworth *et al.*²³ estimated the amount of fluid present as either 9 to 30% fluid-filled porosity, or a total width of 30 m of fluid-filled macroscopic cracks, assuming that the fluid is a brine of 30,000 ppm chloride similar to that found in the deepest drillhole to date near Parkfield. Li *et al.*²⁴ had previously inferred the existence of a seismic low-velocity zone of similar width to model seismic trapped waves in the fault zone. The seismic low-velocity zone would require at least some of the fault-zone fluid to be distributed in pores, rather than localized in cracks.

Studies of gas flux have been made at Parkfield to investigate the hypothesis that CO₂ outgassing from deep sources could provide the fluid pressurization needed to account for low frictional stress across the SAF. Lewicki and Brantley²⁵ measured CO₂ fluxes and concentrations along 16 fault-crossing transects, and found high CO₂ flux anomalies on 12 transects within about 40 m of the fault trace. The high-flux locations, however, were not always the sites of highest CO₂ concentration, and isotopic studies indicate the CO₂ is of biogenic origin. Thus the fault zone represents a high permeability or diffusivity conduit for the escape of biogenic CO₂, with no evidence for deeper degassing. This study, which included transects on Middle Mountain close to the MT profile and directly above the 1966 epicentre, suggests that the fault at shallow depth is a conduit for vertical flow, rather than a low-permeability zone that would help maintain high fluid pressure at depth.

The previous studies show that bodies that might contain fluids are likely present, and that the hydrologic properties of the fault zone are distinct from those of its surroundings. Johnson and McEvilly²² considered how microseismicity features might reveal fluid involvement. The clusters in which similar microearthquakes repeat at fairly regular intervals could be sites of unique fluid pressure, rather than lithologic conditions. Some bursts of localized microseismicity include sequences of hypocentres successively further from the initial event over periods of hours and distances of 1 to 2 km. Although

moment tensor decomposition is problematic for such small events, there are some events with non-double-couple components that indicate flattening of the source. Both features are consistent with hydrofracture of high-fluid-pressure 'pods', and less consistent with failure of isolated impermeable asperities surrounded by a generally high-fluid-pressure fault plane.

Evidence to date for fluid-driven seismicity at Parkfield includes seismic velocities consistent with the presence of fluids in the fault zone, including the 1966 hypocentre, and with additional corroboration from the resistivity structure shallower than 4 km. Seismicity patterns that resemble those expected from diffusion of localized pore pressure have occurred. Gas studies show that at shallow depths, the fault is a zone of relatively high vertical permeability. The sources of fault-zone fluids and the level of *in situ* pressures remain unknown, and are important scientific goals of proposed deep drilling at Parkfield.

5. Departures from steady-state strain accumulation

Roeloffs and Langbein¹ noted few departures from steady-state strain accumulation between 1985 and 1993. This picture has now changed: geodetic and seismic observations show that aseismic fault slip at Parkfield accelerated in late 1992 or early 1993. This tectonic epi-

sode began with increased seismicity, which has since subsided, and continued until 1997 with faster strain rates measured by BTSM's, the 2-colour EDM, and at least one reliable creepmeter. Fault slip rates at depth, inferred using an innovative technique based on the recurrence intervals of repeating microearthquakes, agree strikingly well with the zones of accelerated slip inferred from surface geodetic measurements.

5.1 Increased seismicity

Starting with a *M* 4.6 earthquake in October 1992, seismicity began to increase near the hypocentre of the 1966 Parkfield earthquake. Seismicity rate increased almost ten-fold, primarily at depths greater than 5 km, and by December 1994 there had been four earthquakes with *M* > 4 in the nucleation zone (Table 1). Ruptures in the three largest events propagated toward the 1966 main-shock hypocentre, and their slip zones surround the 1966 hypocentre on three sides^{26,27}. The *M* > 4 earthquakes in this sequence have added at least one bar of stress favouring right-lateral fault slip in the nucleation zone, without triggering or developing into another *M* 6 Parkfield event. Fletcher and Guatteri²⁷ point out that all of these events ruptured either updip or to the NW, whereas numerical simulations²⁸ show that right-lateral ruptures should propagate more easily to the SE because the

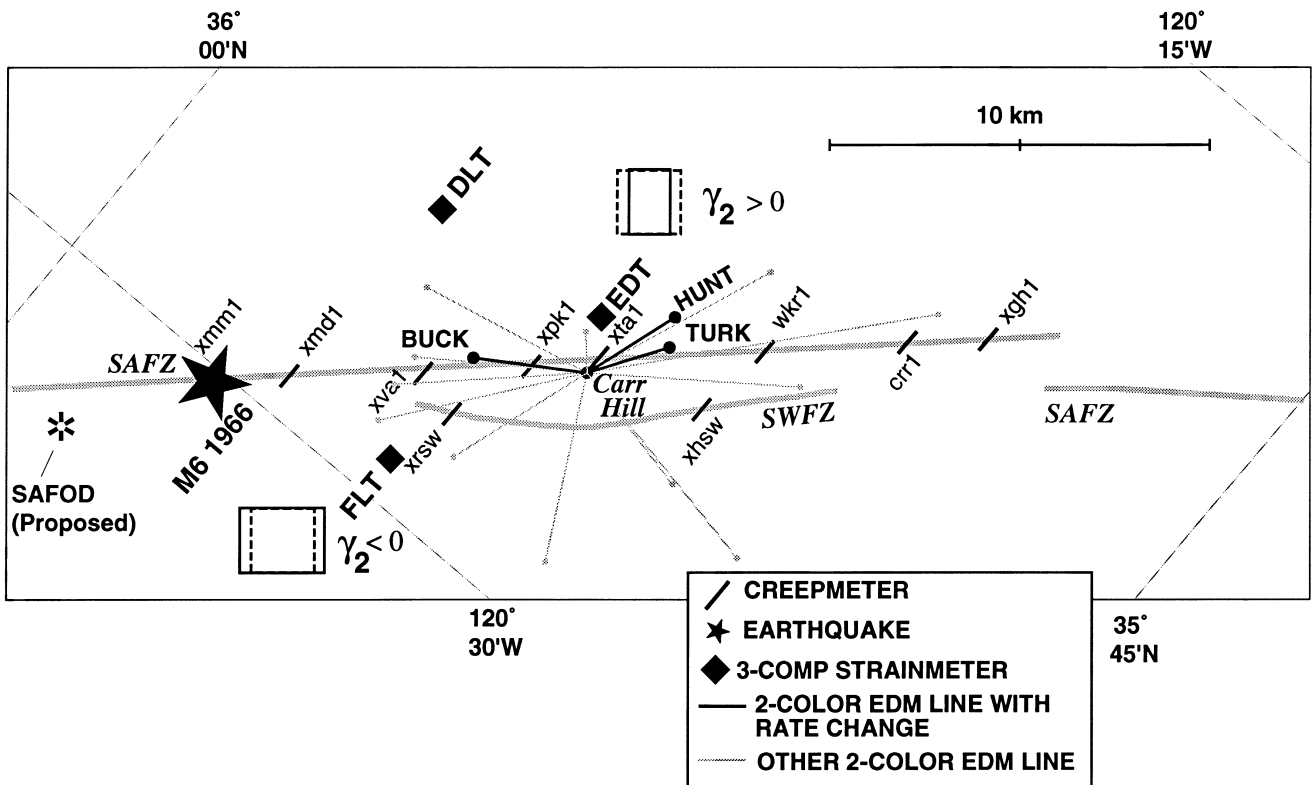


Figure 2. Map of the most densely instrumented segment of the SAF near Parkfield, showing locations of creepmeters, BTSMs and the 2-colour EDM network.

slower material lies NE of the fault. The 1934 and 1966 Parkfield mainshocks both had SE-propagating ruptures, whereas the 1934 and 1966 17-min foreshocks ruptured to the NW⁷.

5.2 Strain and EDM measurements

Changes in the aseismic slip rate became detectable with about two years of additional data. Gwyther *et al.*²⁹ first called attention to changes in the fault-parallel shear strain rates measured by two BTSMs. Since 1993, the NE-striking gages of the EDT and FLT 3-component borehole strainmeters, on opposite sides of the fault (Figure 2), began recording slower extension and slower contraction, respectively, with relative rate changes of 0.1 to $0.5 \times 10^{-6}/\text{yr}$. Figure 3 shows these data as resolved into shear strain components parallel and perpendicular to the fault. Gwyther *et al.*²⁹ modelled the BTSM observations with upward and north-west propagation of a patch of accelerated slip centred beneath EDT (Figure 4).

The observation was initially controversial for two reasons. First, borehole strainmeters clearly work well for observing strain with periods of hours to days, such as coseismic steps or slow earthquakes, but they cannot be used to determine absolute strain rates because of long-term strains induced by curing of the grout in which the instrument is installed, and by creep of the rock in the immediate vicinity of the borehole. The strain rate changes that appeared to have taken place between 1992 and 1993 represent a time scale intermediate to the short periods where the instrument works well, and steady state, where it does not work at all. The second source of controversy was the coincidence of the strain rate change with an increase in annual rainfall. The cumulative annual precipitation could also be viewed as having a rate change between 1993 and 1995 (Figure 3).

The idea that the rate changes could be local to the BTSMs was disproven when measurements made by the two-colour EDM network³⁰ revealed that three fault-crossing, near fault-parallel baselines had begun to lengthen or shorten more rapidly since early 1993. Langbein *et al.*³⁰ modelled the combined BTSM and EDM data sets using a spatially smooth slip rate distribution. This slip rate distribution places the area of greatest slip acceleration to the north-west of EDT and FLT, extending to a depth of at least 5 km, with acceleration of fault slip by as much as 8 mm/year. A shallower area of increased slip rate is inferred beneath the EDM network at Carr Hill.

Gao *et al.*³¹ independently analysed the data from the BTSMs and the EDM network, confirming the rate change. They also noted that the sense of strain at the EDT and FLT BTSMs was inconsistent with accelerated slip limited to the area under Carr Hill, concurring with Langbein *et al.*³⁰ that slip had accelerated even more to the north-west of these instruments.

Faster relative slip since 1993 was also indicated by several creepmeters in Parkfield. Roeloffs³² examined the Parkfield creep data set to determine which instruments characteristically respond to rainfall, and to correct for seasonal variations at several sites. She judged a creep rate increase at CRR1 most likely to be tectonic because it includes discrete steps unrelated to rainfall, and because CRR1 has not exhibited accelerated creep in response to rainfall in the past (Figure 3). The XTA1 creepmeter is closest to the BTSM at EDT, and also shows an increased creep rate since 1993, but has large seasonal signals that prove difficult to remove or explain. Raw data from the XVA1 creepmeter also show faster creep since 1993, but this rate change appears less pronounced when seasonal signals are removed. The northernmost creepmeters (XMM1 and XMD1), directly above the area of greatest inferred slip acceleration^{30,31}, show no acceleration of creep that cannot be attributed to rainfall. Although the XMM1 and XMD1 sites were chosen to span zones of localized right-lateral aseismic slip, the

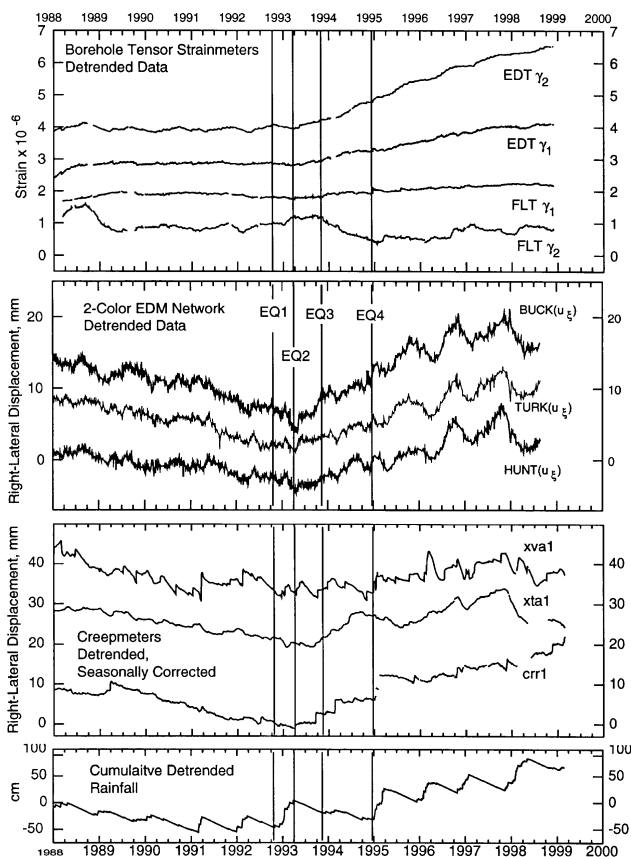


Figure 3. Data from BTSMs, the 2-colour EDM network, and three creepmeters for the period 1985 to 1999. Cumulative rainfall is also shown. All data records have had linear trends removed. Seasonal adjustments have been applied to the creepmeter data as described in Roeloffs³².

1966 Parkfield earthquake produced no surface rupture at those sites, demonstrating that deep accelerated slip may occur with no surface expression on this part of the SAF.

There is concern that variations in soil moisture or groundwater pressure could be affecting not only the creepmeter, but also the strainmeter and EDM measurements. Between 1991 and 1993, groundwater levels began to rise due to increased annual rainfall. Like the creepmeters, the EDM network utilizes surface monuments that could be destabilized by rainfall. The BTSMs are installed about 100 m deep in competent rock, but areal strain is still expected to vary with subsurface fluid pressure, although shear strain should be less strongly coupled. Nevertheless, the simultaneity of the deformation rate changes with deeper seismicity changes argues for a tectonic explanation.

5.3 Deep slip rate inferred from microseismicity

Nadeau and McEvilly³³ developed a method for inferring fault slip rate from the average recurrence interval in each cluster of repeating Parkfield microearthquakes, and showed that the $M > 4$ seismicity during 1992 to 1994 was accompanied by a rather widespread decrease in these recurrence intervals. The increased slip rate first became apparent between April and October 1992, for clusters 9 to 12 km deep and immediately north-west of the 1966 hypocentre. Between October 1993 and April 1994, the zone of accelerated slip propagated upward, covering the rupture area of EQ3 in November 1993.

Between April 1994 and April 1995, the recurrence interval anomaly intensified, covering a zone 2 to 6 km deep and along strike as far as 6 km SE of the 1966 mainshock epicentre. On 20 December 1994, EQ4 occurred near this south-eastern extension of the inferred high-slip-rate zone. Meanwhile, another zone of more rapid slip developed directly beneath Carr Hill at depths of 6 to 10 km, with slip rates 1 to 1.5 cm above average persisting from April 1994 to October 1997.

Figure 4 superimposes the total area of the fault for which Nadeau and McEvilly³³ inferred slip rate increases of 5 mm/year or more on the areas of accelerated slip inferred from the EDM and BTSM data. All studies find a zone of greatly increased slip rate on the fault section north of FLT. Beneath Carr Hill, however, the micro-earthquake recurrence intervals show shortening only in the depth range 7 to 12 km, while the EDM data, and to some extent the creep data, indicate accelerated slip at shallower depths.

Although the accelerated fault slip at Parkfield since 1992 is well-documented, it is not clear what its significance is for the timing of the next $M 6$ Parkfield earthquake. Since 1997, there is some indication in the 2-colour EDM and BTSM data that the rate changes have modified character or returned to their pre-1993 rates (J. Langbein, pers. commun.). Few other measurements exist anywhere to document variations in aseismic strain rate to this level of detail. Strain rate changes before the 1989 Loma Prieta, California earthquake³⁴ and the 1995 Kobe, Japan earthquake³⁵, appear to have continued until a large earthquake took place, and therefore could actu-

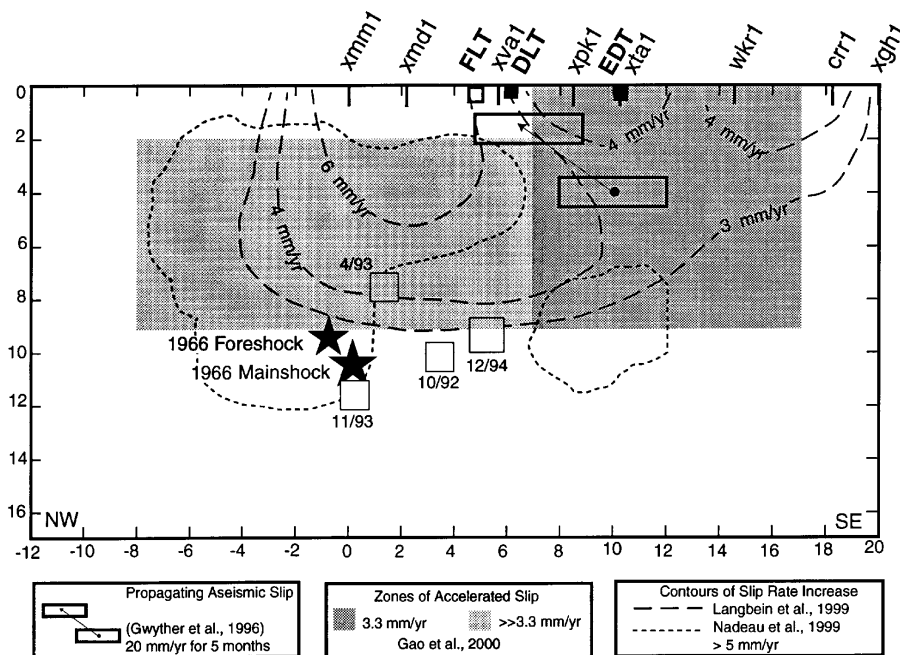


Figure 4. Cross-section of the SAF near Parkfield showing areas inferred to have slipped more rapidly between 1992 and 1997.

ally have been earthquake precursors. But a 'slow earthquake' on the SAF near San Juan Bautista, California³⁶, and the controversial Palmdale, California, uplift episode³⁷ demonstrate that strain rate variations are not always immediately followed by large seismic events.

Although emphasis has been placed on documenting and modelling the strain rate changes at Parkfield, little attention has been called to the magnitude of these changes. The $\dot{\epsilon}$ shear strain rate can be viewed as a measurement of slip rate change along the strike of the fault. Surface creep rate at Parkfield varies approximately linearly with distance, decreasing from 15 mm/yr to zero from NW to SE over the 34 km segment from XMM1 to X461. This creep rate gradient corresponds to a roughly uniform fault-parallel shear strain rate of $\pm 0.22 \times 10^{-6}$ /yr, assuming the strain is divided equally between the two sides of the fault³². $\dot{\epsilon}$ is positive on the NE side of the fault, and negative on the SW side. Thus the observed BTSM rate changes of 0.5 to 0.6×10^{-6} /yr represent accelerations of the background strain rates that amount to an approximate doubling of the along-fault slip gradient, at least locally near FLT and EDT. Inferred subsurface slip-rate changes of 5 mm/yr or more represent increases of at least 25% of the background rate. Thus the slip rate variations, although not greatly above the detection limit of the Parkfield instrumentation, constitute a very sizeable change in the aseismic deformation rate along the SAF.

5.4 Deformation-rate changes and timing of the next *M* 6 earthquake

No *M* 6 Parkfield earthquake has recurred as of April 2000, though a repose interval over 150% of the average recurrence interval has elapsed and a slip deficit larger than the 1966 coseismic offset had apparently reaccumulated several years ago (see summary in Roeloffs and Langbein¹). The increased rate of fault slip since 1993 implies that stored moment is accumulating even more rapidly than the steady rates assumed in the study by Segall and Harris³⁸, which can be thought of as a moment budget balance, and which supported the hypothesis that an *M* 6 earthquake could occur before 1993. Moreover, the factor of three disparity between Parkfield's last two recurrence intervals now appears typical for other locations and tectonic settings as well^{13,39,40}. Statistical analysis of past recurrence intervals and moment-budget balancing based on contemporary deformation rates are mainstays of earthquake probability estimates. Nationwide in the US, probability estimates of this type are multiplied by expected seismic accelerations to obtain probabilities of exceeding specified levels of ground shaking. Seismic building codes based on these probabilities of exceedance are being phased in nationwide. If the detailed data available for Parkfield can reveal why recurrence is irregular and improve techniques for

moment-budget balancing, then direct practical payoffs can be expected in the form of more accurate estimates of earthquake damage probabilities.

Different hypotheses about the earthquake initiation process predict different changes in aseismic deformation rates before the next *M* 6 earthquake at Parkfield, so the documentation of slip-rate variations provides a new and much-needed constraint on these proliferating models. For example, Stuart and Tullis⁴¹ carried out computer simulations presuming earthquake initiation is controlled by laboratory-derived state- and rate-dependent friction, which leads to localized accelerated slip near the 1966 hypocentre preceding seismic fault rupture, and slow shrinkage of the locked portion of the fault as patches near its edge mobilize in the second half of the earthquake cycle. In these simulations, an inflection point occurs for fault creep near the middle of the inter-earthquake period, when slowing creep in the first half of the cycle changes to accelerating creep in the latter half. Stuart and Tullis⁴¹ suggest that this point occurred in 1982–1983, implying that the next *M* 6 event should be due after a recurrence interval of about 34 years. Fitting the model to this deformation-rate curvature, moreover, requires the critical slip distance in the friction law for the locked patch to be about 10 mm. This distance is not too different from the range of 2.4 to 4 mm obtained by Fletcher and Spudich²⁶ from the initial phases of the ruptures of EQ1, EQ3, and EQ4.

Stuart⁴² investigated refinements to this model that could produce the observed variations in aseismic slip rate. He determined that assigning a slightly lower strength to a portion of the locked mainshock patch could cause it to fail earlier, with subsequent aseismic slip in that zone accounting for the observed slip-rate changes. With this model, the mainshock is also expected within the next few years.

An alternative explanation for the current long period of repose was advanced by Miller *et al.*¹⁹, who proposed that seismicity in 1982–1985 north-west of Parkfield in the New Idria–Coalinga–Kettleman Hills region reduced the rate of tectonic compaction normal to the SAF, in turn slowing undrained fluid pressure buildup that could promote fault weakening. Key supporting observations are the onset of seismic quiescence near Parkfield during the New Idria–Coalinga–Kettleman Hills activity, and a possible decrease in the rate of fault-normal contraction between 1984 and 1986. (The change in contraction rate is controversial because it coincides with transition from trilateration to the two-colour EDM network, but could be resolved with further analysis of the geodetic data.) Miller *et al.*'s¹⁹ model presumes that microseismicity reflects slip of individual cells on a steadily sheared fault, occurring when high effective stress is reached within the cell, similar to the model favoured by Johnson and McEvilly²². In simulations, such a system evolves from quiescence to diffuse seismicity to clustering, similar to

temporal changes in Parkfield seismicity between 1982 and 1995. No comparison was made with post-1990 slip-rate variations, however. Large simulated events occur in the model only when the clustering stage has been reached, indicating a strongly heterogeneous shear stress distribution on a fault weakened by widespread high fluid pressure. Miller *et al.*¹⁹ suggest another large event may be possible in the year 2000, and that it may be preceded by foreshocks.

6. Have any earthquake precursors been observed?

Since one goal of the Parkfield experiment is to investigate the possibility of earthquake prediction, and since there have been a number of earthquakes in and around this area since the monitoring began, it is reasonable to ask whether any signals have been detected that could be precursors to earthquakes.

On 4 August 1985, a M_w 6.1 earthquake occurred in the Kettleman Hills area, approximately 35 km NW of Parkfield. The earthquake occurred only a few months after groundwater-level monitoring had started near Parkfield. Roeloffs and Quilty⁴³ later noted that small water-level rises had occurred in two of the four instrumented wells, beginning three days prior to the Kettleman Hills earthquake. A similar change was recorded on one of the two borehole strainmeters then operating at Gold Hill. The water-level change was unique in the data from one of the two wells, but other fluctuations of similar size occur frequently in the other well and in the data from the strainmeter. All four wells had recorded coseismic drops in water level, consistent in direction and size with the static strain field imposed by the earthquake. This observation was submitted to the IASPEI Subcommittee for evaluating proposed precursors to earthquakes, and was admitted as Case 5 to the list of Preliminary Significant Precursors.

The strain and water-level changes prior to the Kettleman Hills earthquake are inconsistent with strain produced by aseismic slip in the direction of the impending earthquake taking place in the immediate vicinity of the mainshock nucleation point, because the pre-earthquake changes were opposite in sign and approximately equal in magnitude to coseismic changes observed in all four wells and both Gold Hill strainmeters. A plausible, but non-unique explanation, would be an aseismic slip event over a portion of the fault surface surrounding the Kettleman Hills mainshock rupture. It is interesting to ask whether slip of this type might precede other earthquakes.

After 1985, no earthquake large enough to produce coseismic water-level changes occurred near Parkfield until EQ4 on 20 December 1994. This event produced coseismic strain changes as large as 0.15 ppm and water-level changes of several centimetres, but no unusual

water-level or strain changes that could be considered precursors. Assuming water-level varies in response to volumetric strain with tidally-derived strain sensitivities on the order of $50 \text{ cm}/10^{-6}$, the coseismic strain changes generally corresponded well with the observed water-level changes⁴⁴. For two sites, however, the coseismic water-level changes were in the right direction but too large, and for one site the change was both too large and in the wrong direction. (Roeloffs⁴⁵ has since shown that at this site, both local and distant earthquakes often induce water-level rises larger than expected on basis of coseismic static strain.) Roeloffs⁴⁶ calculated the amount of slip over subareas of the SAF that would be required to produce 3-cm water-level changes or a strain change of 0.1×10^{-6} , the minimum amounts that could be detected in water-level or strain data if they occurred over a few days prior to EQ4. This exercise showed that if pre-earthquake slip had exceeded 3 to 4 cm over a $4 \times 4 \text{ km}$ fault area at depths of 10 km or less, it should have produced observable water-level or strain changes, but that slip as great as 6 to 11 cm over the same size area could have taken place in the depth range 10 to 14 km without being detected (Figure 5). (The absence of coseismic water-level drops during EQ1 and EQ3 is consistent with these bounds, given the depth and estimated slip distributions of these earthquakes²⁷.) Since the total slip during EQ4 was about 11 cm, pre-earthquake slip larger than this amount would not be expected. Roeloffs⁴⁶ also showed that the water-level rise prior to the Kettleman Hills earthquake was still unique in the data from one of the wells, and that a third dilatometer that had failed to record a pre-earthquake strain was experiencing such rapid contraction from its recent installation that the strain transient would have been undetectable there.

Prior to EQ4, enhanced ultra-low frequency magnetic field variations (0.01 to 10 Hz) were recorded at two stations near Parkfield by Fraser-Smith and Liu.⁴⁷ An upper-atmospheric origin for these signals can be ruled out because they were not observed at other sites in Cali-

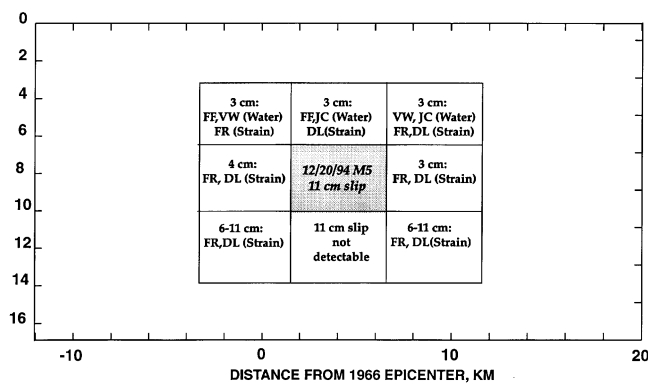


Figure 5. Cross-section of the SAF near Parkfield showing the amounts of slip that could have occurred prior to the 20 December 1994 M 5 earthquake without detection by the water-level and strain sensors operating at that time.

ifornia. These magnetic field variations are the only pre-earthquake changes of any type that could be considered possible precursors to EQ4.

7. Future plans for deep drilling

Important constraints on conceptual models of earthquake initiation are envisioned when scientific drillholes can actually sample active faults at seismogenic depths. Parkfield has been selected as the first site at which to undertake such drilling on the SAF. Funds have been requested from the US National Science Foundation, with additional support from the International Continental Scientific Drilling Program, the USGS, US National Laboratories, and foreign governments, to support drilling into and through the SAF to a depth of 4 km. Nadeau and McEvilly¹⁶ show that a 3-km-deep cluster of microseismicity is a feasible target for the drilling program. Because absolute earthquake locations cannot be obtained with sufficient precision from near-surface measurements, downhole seismic recordings of cluster activity and surface calibration explosions, to be obtained when the drill-hole reaches 2 km, will be used to guide drilling into the microearthquake cluster. Core and fluid samples will be recovered from the borehole, including samples of the fault zone itself. After drilling, long-term instrumentation with seismometers, strainmeters, and fluid-pressure sensors will be initiated. Details of the drilling proposal and progress reports on funding may be obtained at the web site <http://pangea.stanford.edu/~zoback/FZD/>.

8. Summary

Despite the unfulfilled prediction that a magnitude 6 earthquake would hit Parkfield before 1993, state-of-the-art methods for assessing earthquake likelihood still assign Parkfield the highest known probability nationwide of a magnitude 6 or greater earthquake. Although there are more pessimistic estimates of the annual Parkfield earthquake probability, the 'consensus' figure of 10%/yr is viewed by many as justification for continuing monitoring at Parkfield. Probabilities of having the next Parkfield M 6 earthquake given occurrence of a potential foreshock have been revised downward.

Some instruments at Parkfield have stopped working, and some experiments have been discontinued for lack of funds. On the other hand, new technology has also been deployed at Parkfield, such as GPS and broadband seismometers. Many data sets from the experiment are now available to the scientific community via the Internet, and all others may be obtained upon request from individual investigators.

Much has been learned about the SAF from the Parkfield experiment. Events with identical seismograms,

recurring in exactly the same locations, constitute a majority of background microseismicity as well as events with $M > 4$. Geophysical studies find fault zone seismic and electrical properties consistent with high fluid content.

The strain rate at Parkfield changed significantly in late 1992 or early 1993, during a period of relatively high seismic activity. The strain rate change was detectable by BTSMs and the two-colour EDM network, as well as in the recurrence intervals of repeating microearthquakes. Worldwide, no other variation of interseismic deformation rates has been so rigorously substantiated, because years of accumulated data from nearby sensitive instruments are required. Whether or not this strain-rate change turns out to be a precursor to the next M 6 Parkfield earthquake, the knowledge gained about the variation of interseismic strain rates with time has important implications for models of the earthquake process as well as for seismic hazard estimation.

Four $M > 4$ earthquakes have occurred in Parkfield since 1990, with scant evidence of pre-earthquake signals. The largest of these events was not preceded by any water-level or strain changes like those that preceded the 1985 Kettleman Hills, California earthquake. Anomalous electromagnetic signals were observed, however. Funding has been requested to drill a deep borehole to penetrate the SAF and a shallow seismic cluster at Parkfield. The expectation is that with continued monitoring and future deep drilling, Parkfield will provide even more critical new information about earthquake initiation.

1. Roeloffs, E. and Langbein, J., *Rev. Geophys.*, 1994, **32**, 315–336.
2. Bakun, W. H. and Lindh, A. G., *Science*, 1985, **229**, 619–624.
3. Kagan, Y. Y., *Tectonophysics*, 1997, **270**, 207–219.
4. NEPEC Working Group to Evaluate the Parkfield Prediction Experiment, US Geological Survey Open-File Report, 1993, vol. 93–622, p. 19.
5. Michael, A. J. and Jones, L. M., *Bull. Seismol. Soc. Am.*, 1998, **88**, 117–130.
6. Agnew, D. C. and Jones, L. M., *J. Geophys. Res.*, 1991, **96**, 11959–11971.
7. Bakun, W. H. and McEvilly, T. V., *Science*, 1979, **205**, 1375–1377.
8. Meltzner, A. J. and Wald, D. J., *Bull. Seismol. Soc. Am.*, 1999, **80**, 1109–1120.
9. Egbert, G. D., *Geophys. J. Int.*, 1997, **130**, 475–496.
10. Varotsos, P., Alexopoulos, K., Lazaridou-Varotsou, M. and Nagao, T., *Tectonophysics*, 1993, **224**, 269–288.
11. Fraser-Smith, A. C. *et al.*, *Geophys. Res. Lett.*, 1990, **17**, 1465–1468.
12. Park, S. K., *J. Geophys. Res.*, 1997, **102**, 24545–24559.
13. Ellsworth, W. L., in *Urban Disaster Mitigation: The Role of Science and Technology* (eds Cheng, F. Y. and Sheu, M.-S.), Elsevier Science, 1995, pp. 1–14.
14. Cole, A. T. and Ellsworth, W. L., *Seismol. Res. Lett.*, 1995, **66**, 28.
15. Nadeau, R. M., Antolik, M., Johnson, P., Foxall, W. and McEvilly, T. V., *Bull. Seismol. Soc. Am.*, 1994, **84**, 247–263.
16. Nadeau, R. M. and McEvilly, T. V., *Bull. Seismol. Soc. Am.*, 1997, **87**, 1463–1472.
17. Tullis, T. E., *Science*, 1999, **285**, 671–672.

18. Boatwright, J. and Cocco, M., *J. Geophys. Res.*, 1996, **101**, 13895–13909.
19. Miller, S. A. *et al.*, *Nature*, 1996, **382**, 799–802.
20. Eberhart-Phillips, D. and Michael, A., *J. Geophys. Res.*, 1993, **98**, 15737–15758.
21. Michelini, A. and McEvilly, T. V., *Bull. Seismol. Soc. Am.*, 1991, **81**, 524–552.
22. Johnson, P. A. and McEvilly, T. V., *J. Geophys. Res.*, 1995, **100**, 12937–12950.
23. Unsworth, M. J., Malin, P. E., Egbert, G. D. and Booker, J. R., *Geology*, 1997, **25**, 359–362.
24. Li, Y.-L., Leary, P., Aki, K. and Malin, P. E., *Science*, 1990, **249**, 763–765.
25. Lewicki, J. L. and Brantley, S. L., *Geophys. Res. Lett.*, 2000, **27**, 5–8.
26. Fletcher, J. B. and Spudich, P., *J. Geophys. Res.*, 1998, **103**, 835–854.
27. Fletcher, J. B. and Gatterer, M., *Geophys. Res. Lett.*, 1999, **26**, 2295–2298.
28. Andrews, D. J. and Ben-Zion, Y., *J. Geophys. Res.*, 1997, **102**, 553–571.
29. Gwyther, R. L., Gladwin, M. T., Mee, M. and Hart, R. H. G., *Geophys. Res. Lett.*, 1996, **23**, 2425–2428.
30. Langbein, J., Gwyther, R., Hart, R. and Gladwin, M. T., *Geophys. Res. Lett.*, 1999, **26**, 2529–2532.
31. Gao, S., Silver, P. G. and Linde, A. T., *J. Geophys. Res.*, 2000, **105**, 2955–2967.
32. Roeloffs, E., *J. Geophys. Res.*, 2000 (submitted).
33. Nadeau, R. M. and McEvilly, T. V., *Science*, 1999, **285**, 718–721.
34. Gladwin, M. T., Gwyther, R. L., Higbie, J. W. and Hart, R. H. G., *Geophys. Res. Lett.*, 1991, **18**, 1377–1380.
35. Fujimori, K., Yamamoto, T., Otsuka, S. and Ishii, H., *Annals, Disaster Prevention Research Institute, Kyoto Univ.*, 1995, **38**, 287–296.
36. Linde, A. T., Gladwin, M. T., Johnston, M. J. S., Gwyther, R. L. and Bilham, R. G., *Nature*, 1996, **383**, 65–68.
37. Savage, J. C. and Lisowski, M., *J. Geophys. Res.*, 1995, **100**, 12703–12717.
38. Segall, P. and Harris, R., *J. Geophys. Res.*, 1987, **92**, 10511–10525.
39. Sieh, K., Stuiver, M. and Brillinger, D., *J. Geophys. Res.*, 1989, **94**, 603–623.
40. Atwater, B. and Hemphill-Haley, E., *Programs Abstr. – Geol. Soc. Am.*, 1997, **29**, 131.
41. Stuart, W. D. and Tullis, T. E., *J. Geophys. Res.*, 1995, **100**, 24079–24099.
42. Stuart, W. D., *EOS, Trans. Am. Geophys. Union (Supplement)*, 1997, S220.
43. Roeloffs, E. and Quilty, E., *Pure Appl. Geophys.*, 1997, **149**, 21–60.
44. Quilty, E. and Roeloffs, E., *Bull. Seismol. Soc. Am.*, 1997, **87**, 310–317.
45. Roeloffs, E., *J. Geophys. Res.*, 1998, **103**, 869–889.
46. Roeloffs, E., *EOS, Trans. Am. Geophys. Union (Supplement)*, 1997, **78**, S207.
47. Fraser-Smith, A. C. and Liu, T. T., *EOS, Trans. Am. Geophys. Union (Supplement)*, 1995, **76**, F360.

ACKNOWLEDGEMENTS. I thank J. Langbein, A. Michael and W. D. Stuart for providing information about instrumentation status, alert levels and unpublished work. I also appreciate insightful review comments by W. L. Ellsworth and W. H. Bakun.